

Fine Grain of the Neural Representation of Human Spatial Vision

Harvey S. Smallman,^{1,2} Donald I. A. MacLeod,³ Sheng He,^{3,4} and Robert W. Kentridge²

¹Smith-Kettlewell Eye Research Institute, San Francisco, California 94115, ²Department of Psychology, University of Durham, Durham DH1 3LE, United Kingdom, ³Department of Psychology, University of California at San Diego, La Jolla, California 92093, and ⁴Department of Psychology, Harvard University, Cambridge, Massachusetts 02138

It is widely held that in human spatial vision the visual scene is initially processed through visual filters, each of which is responsive to narrow ranges of image spatial frequencies. The physiological basis of these filters are thought to be cortical neurons with receptive fields of different sizes. The grain of the neural representation of spatial vision is much finer than had been supposed. Using laser interferometry, which effectively bypasses the demodulation of the optics of the eye, we measured discrimination of, and adaptation to, high spatial frequency laser interference fringe patterns. Spatial frequency discrimination was good right up to the visual resolution limit

(average Weber fractions of 0.13 at 50 c/deg). Both contrast and spatial frequency matches made after adapting to extremely fine interference fringes strongly suggested that there existed even finer, relatively unadapted, filters (mechanisms with small receptive fields). The smallest cortical receptive fields processing spatial information in human vision are so small that they can possess receptive field centers hardly wider than single cone photoreceptors.

Key words: spatial vision; psychophysics; laser interferometry; adaptation; spatial frequency; visual cortex; receptive field

Twenty-five years of psychophysical and physiological research have led to the view that the retinal image is initially processed through an array of visual filters, or channels, each of which is sensitive to a limited range of image spatial frequencies (Campbell and Robson, 1968; Blakemore and Campbell, 1969; DeValois and DeValois, 1988). The physiological bases of these filters are thought to be cortical neurons with different receptive field sizes (DeValois et al., 1982). What are the characteristics of the finest foveal channel? What is the finest grain at which the image is neurally represented?

Contemporary models of pattern vision differ in number, center spatial frequency, and spacing of channels (Watson, 1983; Wilson et al., 1983; Klein and Levi, 1985; Watt and Morgan, 1985). In one particularly well known model, developed primarily to account for spatial frequency masking data taken up to 22 c/deg, there are six spatial frequency-tuned channels (Wilson et al., 1983; Wilson, 1991). The finest foveal channel in this model is centered at 16 c/deg. On this account, it alone mediates perception of frequencies from 16 c/deg up to the visual resolution limit. It possesses an excitatory receptive field center of ~ 1.9 arc min (Wilson, 1986). This would correspond on the retina to a mechanism with a receptive field center spatially integrating over more than three foveal cones. Physiological evidence suggests, however, that a much finer signal is transmitted up the optic nerve. There are between one and four ganglion cells per primate foveal cone (Perry and Cowey, 1985; Schein, 1988), and some foveal ganglion cells and

lateral geniculate nucleus (LGN) cells have receptive field centers fed by single cones (Polyak, 1941; Boycott and Dowling, 1969; DeMonasterio and Gouras, 1975; Derrington and Lennie, 1984; Dacey, 1993; McMahan et al., 1995). Further, there is evidence that the fovea is relatively overrepresented in the cortex (Azzopardi and Cowey, 1993). All of this evidence suggests that an extremely fine spatial (high frequency) signal is available to cortical processing. In the cortex, our knowledge of the fine-grain visual representation is hazy, partly because of the severe technical problems involved in such research. So far no one has reported cortical receptive fields fed by single cones. The highest reported preferred center spatial frequency for a cortical cell is 24 c/deg in vervet monkey V1 layer IVc β (Parker and Hawken, 1985), and in a larger sample of macaque striate cells the highest was 16 c/deg (DeValois et al., 1982).

Channels have been characterized with a variety of psychophysical techniques including detection, discrimination, masking, and visual adaptation (Graham, 1989). Nearly all of this work has been conducted at frequencies of 32 c/deg, even though the resolution limit for foveally presented gratings is nearly twice this frequency (60 c/deg) (Campbell and Green, 1965; He and MacLeod, 1995). The reasons for this are twofold: (1) the modulation transfer function (MTF) of visual displays makes it inconvenient to present high-contrast high-frequency stimuli; and more important, (2) the MTF of the eye itself makes it impossible to conventionally present high spatial frequency targets with enough retinal contrast to use classic psychophysical procedures such as contrast adaptation. We have investigated the fine grain of spatial vision using a technique that allows for the presentation of very high spatial frequency patterns. Our stimuli were interference fringes generated with a laser interferometer, which essentially allows the optics of the eye to be bypassed (Campbell and Green, 1965; Williams, 1985a; MacLeod et al., 1992). We demonstrate three perceptual correlates of signals that come from underlying channels so fine that they must be attributable to cortical receptive

Received Aug. 7, 1995; revised Dec. 6, 1995; accepted Dec. 7, 1995.

This work was supported by National Institutes of Health Grant EY01711, by the Royal Society, and by the Smith-Kettlewell Eye Research Institute. We thank Drs. Stuart Anstis, Julie Harris, and Suzanne McKee for comments on a previous draft of this manuscript.

Correspondence should be addressed to Harvey S. Smallman, Department of Psychology, University of Durham, Science Labs, South Road, Durham DH1 3LE, UK.

Copyright © 1996 Society for Neuroscience 0270-6474/96/161852-08\$05.00/0

field centers fed by slightly more than the width of single foveal cones.

Some of this work has been reported previously in abstract form (He et al., 1995).

MATERIALS AND METHODS

All observations were conducted on the recently completed six-channel UCSD laser interferometer (for review, see He and MacLeod, 1995). Interferometry was introduced into vision research by LeGrand (1935) as a technique to allow the optical attenuation resulting from the diffraction limit of the pupil to be bypassed. Modern laser interferometry allows for patterns of exceptionally high spatial frequency to be presented with almost unity retinal contrast (Williams, 1985a; MacLeod et al., 1992). Our observers, on bite bars, monocularly fixated the center of a 5° bipartite field in a dark surround. Vertical laser interference fringes, the spatial frequency and contrast of which were under computer control, were introduced, filling both half-fields, for 400 msec every 5 sec. The task of our observers was to match the perceived contrast and spatial frequency of the sinusoidal fringe patterns in the lower (test) half-field with interference fringes filling the top (comparison) half-field. This they did with a hand-held trackball. By rolling the trackball in one axis, they could modulate the spatial frequency of the comparison fringes with fine precision, and by rolling it in the other axis they could change their contrast. After as many series of 400 msec “glimpses” of their matches as it took to satisfy them that they were acceptable, they clicked a mouse button and the next trial was initiated.

The 5 sec interval between presentations was either uniform or contained adapting fringes. These adapting fringes were presented only in the lower half of the bipartite region and were of unity contrast and of various spatial frequencies. Unless otherwise stated, all reported data were taken with unity test contrasts and adapting contrasts, where Michelson contrast, C , was conventionally defined to be

$$C = \frac{L_{\max} - L_{\min}}{L_{\max} + L_{\min}}$$

(where L_{\min} and L_{\max} were the maximum and minimum luminances, respectively). However, further data taken with lower test contrasts of 0.25–0.75 lead us to trust the generality of the results reported here. A single experimental run involved an observer making a series of six matches for each test spatial frequency, for a range of test frequencies. After each match was accepted, the computer reset the contrast and spatial frequency of the comparison region to random values and the observer had to start again. The observer made three matches consecutively at the lowest test frequency and then three at the next highest, and so on, until they reached the highest test frequency. Then the sequence was repeated with test frequency going back down the range, and three matches were made again at each test frequency. Matches were made for test frequencies ranging from 3 c/deg up to 52 c/deg.

The helium–neon (He–Ne) laser had a wavelength of 632.8 nm. The space average luminance of the field was maintained at 4800 td. It appeared a uniform red when the contrast of the interference fringe patterns was zero, apart from inevitably present minor laser speckle. At high spatial frequencies, high-contrast fringes appeared desaturated, a phenomenon that has been reported previously (Campbell and Green, 1965), and which probably is attributable to some early saturating non-linearity (MacLeod and He, 1993; He and MacLeod, 1995). Although the field diameter was 5°, at the highest spatial frequencies used here fringes could only be seen at the very center of gaze even when presented with the highest contrast.

Three observers took part in the study. Two observers were co-authors of this paper (S.H. and H.S.S.), and the third (R.C.) was unaware of the purposes of the study. Observer S.H. possessed several years experience of inspecting interference patterns, whereas the other two observers had far less exposure.

RESULTS

The results of the experiment were a series of matches of test interference fringe patterns of various spatial frequencies and contrasts both in the absence of, and after adapting to, interference fringe patterns of other spatial frequencies. Presentation of results is divided into three sections.

Spatial frequency discrimination

The variability in an observer's matches along a stimulus dimension can be considered an estimate of an observer's ability to discriminate along that stimulus dimension. So in the case of spatial frequency, the SD of a series of grating matches at a given test spatial frequency, f , can be considered an estimate of grating discrimination threshold, or Δf (Campbell et al., 1970). We measured spatial frequency discrimination from 3 c/deg up to the highest spatial frequencies that subjects could resolve. Figure 1*b* shows the Weber fractions ($\Delta f/f$) for discriminating the higher spatial frequencies (>10 c/deg), in the absence of adaptation, as a function of test spatial frequency for three observers. This is the first time that this function has been measured without the attenuation imposed by the optics of the eye. It had only been measured previously up to 30 c/deg, and in that study had been shown to be fairly independent of frequency across that range, averaging ~0.05 (Campbell et al., 1970). Later studies that examined discrimination over a narrower range of frequencies (1–20 c/deg) have confirmed that the function is fairly constant across frequency, with Weber fractions ranging from 0.02 to 0.05 (Hirsch and Hylton, 1982; Regan et al., 1982). In agreement with these earlier studies, but with a radically different methodology, we find that the Weber fraction for spatial frequency discrimination ranges from 0.02 to 0.04 at low spatial frequencies (<24.5 c/deg). However, what is notable is that the Weber fractions are low even at extremely high spatial frequencies. Frequency discrimination only starts to become impossible near the visual resolution limit. There were some differences here between the more experienced observer, S.H., and the other two observers who had less experience with laser interferometry, H.S.S. and R.C. Discrimination fell off dramatically (Weber fractions of >0.25) for those two observers at ~52 c/deg, whereas S.H. could still discriminate a 10% change in spatial frequency at this test frequency. Interestingly, expressed as a fractions of grating cycles on the retina, S.H.'s discrimination thresholds at high spatial frequencies are remarkably good, with the best at 32.7 c/deg of 3.5 arc sec, or one-ninth the width of a single foveal cone (Williams, 1988), thus placing them in the hyperacuity range (Westheimer, 1981).

These data strongly imply that there are mechanisms tuned to very high spatial frequencies operative in human spatial vision. To demonstrate why this is so, we show here how spatial frequency discrimination can be simply related to the responses of a set of spatial frequency-tuned mechanisms. We show why the ability to discriminate among very high spatial frequencies means that there must be mechanisms tuned to higher spatial frequencies.

To model the data with a set of channels, it was necessary to know the contrast sensitivity function (CSF) for neural resolution losses under similar experimental conditions. The most comparable CSF was determined recently with the same apparatus at a mean luminance level of 1000 td by He and MacLeod (1995). Data are shown from that study. Average contrast sensitivity (reciprocal of 84% contrast thresholds) of observers S.H. and D.M. for discriminating small differences in orientation ($\pm 10^\circ$ from vertical) with interference fringes of different spatial frequencies is shown in Figure 1*a* (solid symbols). On the same graph (solid lines) is shown the best fit of the top two foveal channels of Wilson's six-channel model of spatial vision (Wilson et al., 1983) at capturing this curve. Because our data were taken without the optics of the eye attenuating the contrast of the high spatial frequency stimuli, it was necessary to divide the sensitivities of the channels at each frequency by the MTF of the eye at those

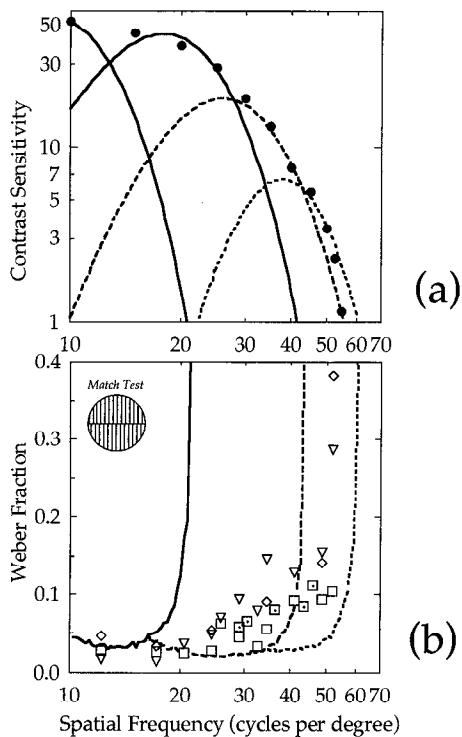


Figure 1. Spatial frequency discrimination and contrast sensitivity for interference fringe patterns of high spatial frequency suggest that mechanisms tuned to high spatial frequencies mediate that perceptual performance. *a*, Contrast sensitivity for discriminating subtle changes in orientation with interference fringe stimuli as a function of their spatial frequency, and the spatial frequency-tuned channels thought to underlie that detection. Reciprocal of contrast thresholds for discriminating $\pm 10^\circ$ from vertical with interference fringes (defined as contrast sensitivity) averaged across the two observers S.H. and D.M. is shown in *solid symbols* on the y-axis (data from He and MacLeod, 1995). The x-axis plots spatial frequency. *Solid lines* on the same graph show the best effort of the top two foveal channels of Wilson's six-channel model of spatial vision (Wilson et al., 1983) at capturing this curve. Two finer channels (*dashed lines*) when added show a better fit to the contrast sensitivity data than Wilson's alone. They are based on the Cauchy functions of Klein and Levi (1985). The lower channel (*large dashes*) is an 8th order Cauchy function centered at 23.4 c/deg with the optics of the eye put back in place. The highest channel (*finer dashes*) is a 16th order Cauchy function centered at 35 c/deg with the optics of the eye put back in place. We make the assumption (which is the usual implicit assumption in the literature) that the channel structure for spatial frequency is homomorphic across spatial frequency. *b*, The ability of observers to discriminate between interference fringe patterns of different spatial frequencies. The y-axis plots the Weber fraction for frequency discrimination, which is the fractional change in frequency required to be discriminable ($\Delta f/f$). Δf was the SD of six matches at a given test spatial frequency (see *inset*). The x-axis plots the test spatial frequency, *f*. The different *symbols* plot the data for three different observers (\square , S.H.; \diamond , H.S.S.; ∇ , R.C.). All of these data were taken with unity test contrasts. Also shown with the *dotted symbol* are further data taken by observer S.H. with test contrast set to 0.75. Frequency discrimination does not become impossible until the visual resolution limit. Modeling of spatial frequency discrimination shows why these data imply that there are mechanisms tuned to very high spatial frequencies in human vision. The *lines* plot the predicted spatial frequency discrimination from the ratio model of discrimination (described in the text) for different combinations of the spatial frequency channels from *a*. On this account, observers are assumed to be basing their discrimination on the noisy ratios of adjacent channel outputs. The *solid line* plots the predicted discrimination performance based on the outputs of the top two channels of the model of Wilson et al. (1983). Note that predicted discrimination performance declines precipitously when the penultimate channel falls below its contrast threshold (see *a*). In *large dashed lines* is shown predicted discrimination performance based on the outputs of Wilson's top channel and the channel shown in the same dash from *a*, which is centered at 23 c/deg.

frequencies before fitting them. We used the recently determined MTF of Williams et al. (1994) because their conditions were most similar to ours; they used laser interferometry and a He-Ne laser. Dividing channel sensitivities by the MTF before fitting them to the CSF data had the effect of shifting the apparent preferred center spatial frequencies of the high channels (especially) to slightly higher spatial frequencies [for review, see Hawken and Parker (1991) for some examples of this effect in action]. Wilson's top two channels fail to capture the interferometric sensitivity above ~ 40 c/deg, which is the first indication that higher channels may exist in human foveal vision.

Spatial frequency discrimination is commonly modeled by assuming that the observer can discriminate between two gratings of different spatial frequency if they give rise to a noticeably different pattern of response across an array of spatial frequency-tuned channels (Campbell et al., 1970; Regan and Beverley, 1983; Watson, 1983; Wilson and Gelb, 1984; Yager and Kramer, 1991). These models differ, however, according to which aspects of the neural representation they consider the observer to be using in making the discrimination. In the well known line element model of spatial frequency discrimination by Wilson and Gelb (1984), each of two test gratings is seen through an array of six mechanisms responsive to different ranges of spatial frequency. The response of each channel then passes through a nonlinear contrast-response function to yield a channel activity. Thresholds for discriminating two gratings are proportional to the vector difference in six-dimensional space of these channel activities to the two gratings. We computed the predictions of a simple version of this model that used only spatial frequency information and found that model predicted good discrimination thresholds up to ~ 40 c/deg, after which predicted discrimination thresholds fell apart precipitously, because the highest channel approached its own contrast threshold. However, this model is unrealistically favored at frequencies above ~ 20 c/deg, because above this frequency the penultimate channel falls below its own contrast threshold and, consequently, would be silent (see Fig. 1*a*). Hence, on this account, changes in contrast would be confused with changes in spatial frequency because there is only one channel changing its response to the high-frequency test gratings. Because of this, we have implemented another simple method of determining frequency discrimination from a set of spatial frequency channels.

The spatial frequency of a grating can be determined, in principle, from the responses of two channels with approximately Gaussian-tapered overlapping sensitivities to spatial frequency by taking the ratio of the logarithms of the two responses. We say that observers rely on changes in this ratio to discriminate the spatial frequency of different test gratings. The model does not confuse changes in contrast with changes in frequency because taking a ratio has the advantage of normalizing away any contrast differences between different gratings. We assume that the discrimination of frequency is perturbed by Gaussian noise injected into the outputs of each channel before the ratio of logarithms is

Discrimination is now possible up to ~ 40 c/deg, which is again where the penultimate channel falls below threshold. The *smallest dashed line* shows the predicted performance of the top two dashed channels from *a*. The same two parameters controlled all model simulations. All were generated with Gaussian noise of SD = 0.1 in this figure, and all of the predicted discrimination functions curves were multiplied by the same gain of 15. The top two added channels were presumed to pass through the same contrast response nonlinearity that Wilson et al. (1983) deduced for their top channel.

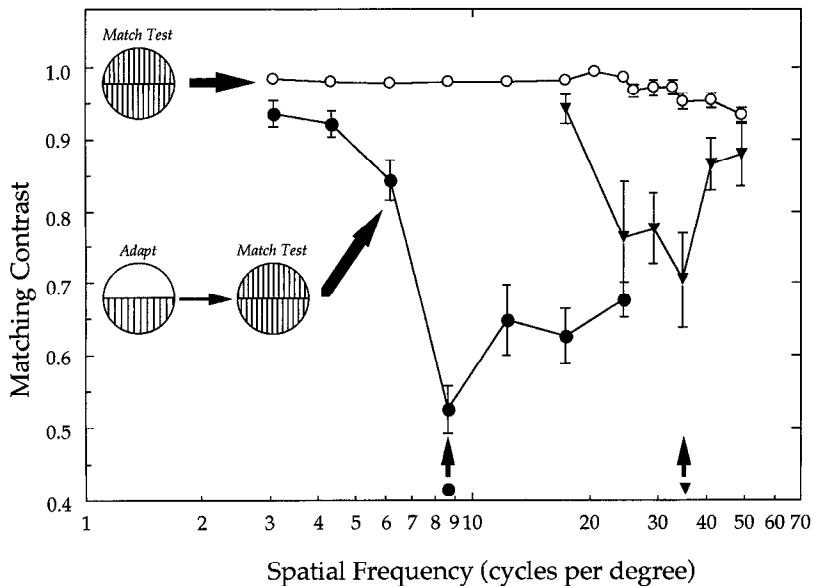


Figure 2. Contrast matching before and after adaptation to interference fringes (see inset) for observer R.C. as a function of the spatial frequency of test fringes. The observer's match to unity contrast test fringes with no adaptation is shown in open symbols. The matches to the same test fringes after adaptation to two different fringe frequencies (shown by arrows at bottom) are shown in solid symbols. The effect of adaptation in both cases was to maximally reduce the contrast of test fringes near the adapting frequency, and to largely spare the contrast of higher and lower test frequencies. This suggests that in both cases there are relatively unadapted mechanisms tuned to spatial frequency, which are centered at higher spatial frequencies than the adapting frequency, that contribute to perceived spatial frequency. The finest channel in human vision is therefore centered higher than 34.5 c/deg.

taken. Because the resulting noise distribution can be shown to have bounded variance provided the difference between the outputs of the channels is much greater than the variance of the injected noise (and that any extremes of noise producing negative sensitivity are clipped), the central limit theorem guarantees that the distribution of the sum of repeated independent samples from this noise will be Gaussian and, hence, the model is compatible with analysis by Signal Detection Theory (Green and Swets, 1966). We can then use Signal Detection Theory to calculate that spatial frequency, which is just noticeably different from another. When either channel in numerator or denominator of the ratio approaches its contrast threshold, changes in the noise cause dramatic changes in the ratio and, therefore, frequency discrimination becomes impossible. The just noticeably different frequency Δf for Wilson's top two channels has been calculated as a function of spatial frequency, f , and the ratio $\Delta f/f$ is plotted alongside the human data in Figure 1b (shown with the solid curve). Inspection of the solid curve in Figure 1b reveals that predicted frequency discrimination now falls apart when the penultimate spatial frequency channel of Wilson's model drops below its contrast threshold (compare Fig. 1a), at ~ 20 c/deg. But the human discrimination data do not start to deteriorate markedly until over an octave higher in spatial frequency. Hence, there must be higher spatial frequency channels. Our quantitative model is similar to an idea put forward by Regan and Beverley (1983).

Two candidate channels, both of which model the CSF and the discrimination data better than Wilson's alone, are shown in Figure 1a (plotted in dashed lines). They are modeled on the Cauchy functions of Klein and Levi (1985). Predicted spatial frequency discrimination as a result of adding these channels to Wilson's original model can be seen in Figure 1b. The simple addition of a channel centered at just over 23 c/deg allows both the CSF and all but the highest frequency discrimination data to be handled better. Note that spatial frequency discrimination falls apart for this model when the lower channel (now Wilson's top channel) falls below its contrast threshold (~ 40 c/deg). But to accommodate the highest frequency discrimination data and adaptation data that we now report, it was necessary to add an additional higher-frequency channel, centered, with the optics of the eye in place, at 35 c/deg.

Contrast matches made after adaptation

It is well known that the perceived contrast of test gratings is reduced by previous viewing of high-contrast adapting gratings, but this only happens over a range of test frequencies around the adapting frequency (Blakemore et al., 1971, 1973; Georgeson, 1985). This is naturally accommodated in a multiple spatial frequency channel model by assuming that perceived contrast at a given test frequency is monotonically related to channel activity at that frequency. Further, if it is assumed that the effect of adaptation is to reduce the activity of those channels that were sensitive to the adapting stimuli to subsequently presented test stimuli, either through adverse neuronal fatigue (Maffei et al., 1973; Albrecht et al., 1984) or through adaptive gain control (Ohzawa et al., 1985; Määtänen and Koenderink, 1991; Wilson and Human-ski, 1993), then adaptation would produce a "notch" in channel activities. This notch manifests itself psychophysically in the reduction of perceived contrast of the nearby test frequencies. Central to the present study is the fact that this logic only applies to the case in which channels of peak preferred spatial frequency exist above and below the adapting frequency. If there were no channels centered at higher frequencies than the adapting frequency, then perceived contrast would be reduced for all test frequencies higher than the adapting frequency. This is because perceived frequency would be determined primarily by the activity of the highest spatial frequency channel for those higher test frequencies, and this is the channel that would be most affected by adaptation; thus, all higher test frequencies than the adapting frequency would appear reduced in contrast.

Contrast matching of test fringe gratings before and after adaptation are shown for observer R.C. in Figure 2. This figure shows the effect of adapting to unity contrast fringes of 8.5 and 34.5 c/deg on the perceived contrast of unity contrast test fringe patterns of different spatial frequencies. Open symbols show the matches before adaptation, which are, of course, close to veridical. However, after adaptation, perceived contrast was reduced over the range of test gratings. Reduction was maximal (with perceived contrast almost halved) for test gratings equal to the adapting grating frequency. Of central interest, however, is that the effect of adaptation was to create a notch in perceived contrast in both cases. The perceived contrast of finer test gratings than the adapt-

ing grating recovers at frequencies higher than the adapting grating, i.e., there was less reduction in perceived contrast in the two finest test frequencies of 41 and 49 c/deg than there was at 34.5 c/deg. Thus, there must be channels centered at higher frequencies than that of our highest adapting frequency of 34.5 c/deg that are less affected by adapting to this frequency than the next lowest channel. This result reinforces our conclusions of the discrimination data presented in Figure 1. We obtained the same effect in the other observers and found even more pronounced losses of perceived contrast when using lower test contrasts of 0.25–0.75.

Spatial frequency matches made after adaptation

More support for the existence of channels with higher preferred spatial frequencies than our finest adapting grating comes from spatial frequency matching after adaptation. It is well known that previous inspection of a stimulus causes the perceived quality of subsequently presented test stimuli to shift away from the adapting stimuli along that perceptual dimension (Anstis, 1975). So in the domain of spatial frequency, prolonged inspection of a fine grating makes even finer gratings appear finer still (Blakemore and Sutton, 1969). This is the familiar “spatial frequency shift.” This phenomenon is well handled in a multiple spatial frequency channel model by supposing that the output of the neural representation that is responsible for coding perceived spatial frequency is the center of gravity or moment of channel activities (Georgeson, 1980). Moderate adapting frequencies create notches in channel sensitivities (as discussed above), and this causes the moments of activity of test stimuli near the adapting frequency to shift away from their positions before adaptation, thus causing the perceptual shift [see Anstis (1975) and Braddick et al. (1978) for good reviews].

In Figure 3 the ratios of spatial frequency matches to veridical matches after adapting to three different high spatial frequency fringe frequencies (17, 25.5, and 34.5 c/deg) are shown for two observers. All data for both observers lie in opposite quadrants of the graphs. Thus, in all cases the effect on test gratings was to make lower test gratings appear lower still in perceived spatial frequency and higher test gratings appear higher still. Thus, the data support the idea that adaptation created a notch in the underlying channels and that this applies for all adapting gratings. Again, if adaptation created a notch in channel sensitivities, then this implies that there must be channels centered higher in frequency than the adapting grating. These higher channels must be relatively unadapted after the subject is exposed to 34.5 c/deg fringes and, therefore, mediate a shift in perceived spatial frequency.

To reinforce the point, note that a model with only lower frequency channels, like Wilson’s, must predict the opposite effect of adaptation to the 34.5 c/deg fringe patterns to that observed (in fact, it must predict the reversed effect for all three adapting frequencies used here). This is because adaptation at these high frequencies would not create a notch in channel activity but, instead, they would be seen by only, and hence would desensitize only, the highest channel centered at 16 c/deg. This would cause a reduction in perceived frequency of subsequently presented higher test gratings and actually make them regress back perceptually toward the adapting grating frequency. Interestingly, such perceptual regressions have been reported recently in the domain of stereopsis after adaptation to large binocular disparities (Smallman and MacLeod, 1994).

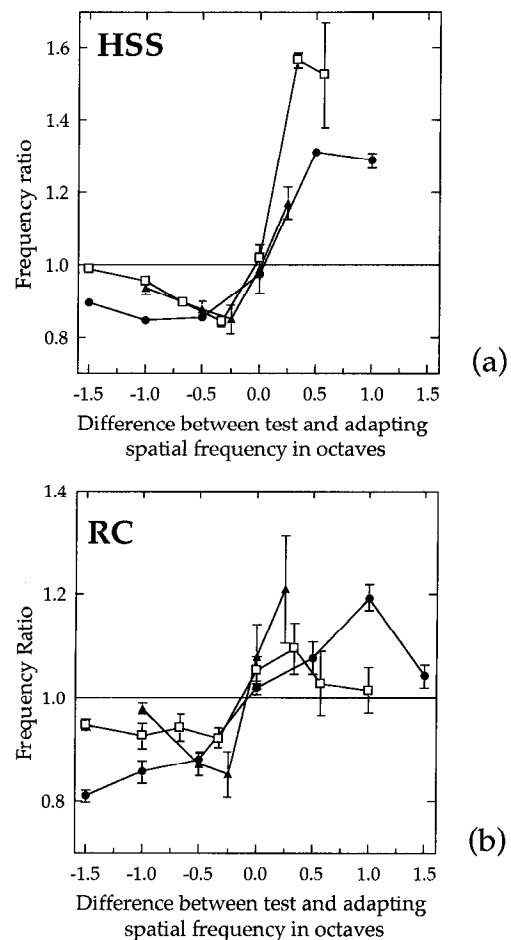


Figure 3. Spatial frequency matching before and after adaptation to interference fringes for two observers (H.S.S. in *a* and R.C. in *b*). The ratio of the matching frequency to veridical spatial frequency (note slight difference in scale for the two observers) is shown on the y-axis. The x-axis plots the difference in spatial frequency between the test and adapt spatial frequency in octaves. There were three different adapting frequencies (●, 17 c/deg; □, 25.5 c/deg; ▲, 34.5 c/deg). Test and adapting contrasts were unity. The effect of adaptation in all cases was to shift the perceived spatial frequency of test fringes so that lower-frequency tests than the adapting one appeared lower still, and higher-frequency tests appeared higher still. This suggests that in all cases there are relatively unadapted mechanisms centered at higher, and lower, spatial frequency than the adapting frequency that contribute to perceived spatial frequency. The finest channel in human vision is centered at higher than 34.5 c/deg.

DISCUSSION

We have demonstrated three lines of evidence for an exquisitely fine grain to the neural representation of human vision—so fine, in fact, that certain cortical receptive field centers are fed by hardly more than the width of single foveal cone photoreceptor. First, spatial frequency discrimination with interference fringe patterns of very high contrast is good right up to the visual resolution limit. We developed a simple ratio model of discrimination to show that high spatial frequency mechanisms are needed to accommodate these data. Second, the perceived contrast of very fine test fringes is less reduced by adaptation to 34.5 c/deg adapting fringes than is the contrast of lower test spatial frequencies near 34.5 c/deg. These data, which we measured by pairing laser interferometry for the first time with the classic psychophysical techniques of pattern adaptation, suggest that the effect of adaptation was to spare the sensitivity of some mechanisms tuned

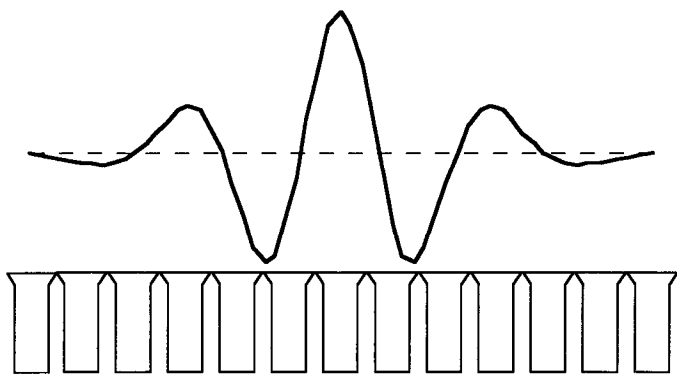


Figure 4. The receptive field of the finest channel in human vision shown above a schematic human foveal cone mosaic of intercone spacing 0.536 arc min (Williams, 1988). The receptive field center is fed by slightly more than one cone. The receptive field is based on a 16th order Cauchy function (Klein and Levi, 1985) with center spatial frequency, with the optics of the eye in place, of 35 c/deg. The tuning of this channel to spatial frequency when exposed to laser interference patterns can be seen in Figure 1a in fine dashed lines.

to higher spatial frequencies. Third, the perceived periodicity of very fine test patterns is shifted to appear even finer still after adapting to 34.5 c/deg test fringes. This result, like the second, suggests that there are relatively unadapted channels tuned to even higher frequencies than 34.5 c/deg.

Figure 1a showed that by adding two additional channels to Wilson's model, we could capture the main trends of the contrast sensitivity data of He and MacLeod (1995) as well as our spatial frequency discrimination data. Because it peaks at such a high frequency when tested with interference fringes, the finest channel of Figure 1a could account for the adaptation data reported in Figures 2 and 3, especially if we assume that it would be difficult to adapt because of its low absolute contrast sensitivity. The finest channel possessed a peak sensitivity of 43 c/deg when tested and adapted with laser interference fringes. But with the optics of the eye back in place, it would appear to peak at 35 c/deg. The reason for this downward shift is that the MTF of the eye can fall faster at high spatial frequencies than does the tail of the sensitivity of a channel (for review, see Hawken and Parker, 1991).

The finest channel has been transformed from frequency back to space in Figure 4. It is shown on top of a schematic one-dimensional human foveal retina of intercone spacing of 0.536 arc min (Williams, 1988). It ripples in space considerably, possessing more than the typically reported three or four discrete subregions, because it must be narrow in frequency to satisfy the constraints of the data—that the channel peaks at higher than 34.5 c/deg and has a sharp cutoff at the visual resolution limit of just under 60 c/deg (He and MacLeod, 1995). This endows it with a comparatively narrow bandwidth of 0.87 octaves at half-height. This is not physiologically unreasonable, however, because periodic cells have been reported in macaque (DeValois et al., 1985). The range of reported bandwidths in a population of >200 macaque striate cells was 0.5–2.5 octaves (DeValois et al., 1982). It is also the case that cells tuned to higher spatial frequencies tend to be narrower-band cells (DeValois et al., 1982), and this is also true of the channels invoked to model psychophysical masking and adaptation data in humans (Wilson et al., 1990). The finest cortical cell yet reported in the literature, by Parker and Hawken (1985), peaked at 24 c/deg. There must be finer cells still to account for our 25.5 and 34.5 c/deg adaptation data. There have

been previous suggestions that Wilson's top channel might be centered too low (Marr et al., 1980) and some data suggesting that there may be channels centered at higher frequencies (Watson, 1982). Morgan and Ward (1985) had suggested previously that Wilson's top channel must be centered too low because they found low separation thresholds with stimuli that should have been impossible to discriminate with those channels because of random "jitter" introduced into the outputs of all of them. However, Wilson (1986) presented simulations of the Morgan and Ward (1985) stimuli and claimed that they would give rise to enough modulation of the 16 c/deg mechanism to model Morgan and Ward's thresholds.

We can be confident that the effects we have reported are cortical in origin because contrast adaptation is found in striate cells (Maffei et al., 1973; Albrecht et al., 1984; Ohzawa et al., 1985) but not in LGN or ganglion cells (Movshon and Lennie, 1979; Derrington and Lennie, 1984; Ohzawa et al., 1985). Cortical contrast adaptation is also implied from the spatial frequency selectivity of our effects, and from the orientation selectivity and interocular transfer of contrast reduction and the spatial frequency shift from older literature (Blakemore and Nachmias, 1971; Blakemore et al., 1973), which are all properties that LGN cells lack but cortical cells possess (DeValois et al., 1977; Wilson et al., 1990).

The fact that the receptive field center is so small shows that there can be very little neural convergence in central fovea in human vision before cortex. This is remarkable when one considers that there are so many sites before cortex where convergence is possible and where it has been indicated. For example, in the retina gap, junctions between photoreceptors might have served to blur the signal from adjacent foveal cones together (Raviola and Gilula, 1973; Tsukamoto et al., 1992). Polyak (1941) suggested half a century ago the existence of what he termed "private lines" between single cone photoreceptors and single ganglion cells based on extensive Golgi staining research. Later it was strongly hinted that there were receptive fields fed by single cones in the optic nerve and LGN (Boycott and Dowling, 1969; DeMonasterio and Gouras, 1975; Derrington and Lennie, 1984; Dacey, 1993). This has very recently been elegantly and unequivocally demonstrated in macaque P cells by McMahon et al. (1995) using laser interferometry. These authors showed that many foveal cells could be driven by fringes of >100 c/deg; the MTF of a single foveal cone aperture can extend out to 150 cpd (Miller and Bernard, 1983). The MTF of our putative highest human cortical cells cuts out at the lower frequency of 60 c/deg, at the visual resolution limit. But our results do complement those of McMahon et al. (1995) by showing that there can be remarkably little neural convergence even in cortex.

We consider here, and reject, three potential objections to our conclusions. First, aliasing artifacts. Williams (1985a) showed with laser interferometry that subjects can see the aliases of fine fringe patterns with their own cone mosaics. Because these aliases are presumed to occur at the very input to the visual system, they might inject spatial frequency components into the image that might have some ability to mask in a frequency-selective manner and hence, it might be argued, influence our results. We restricted our observations to frequencies below the resolution limit, at which our 5° field was small enough to ensure that they were never visible (for review, see Williams, 1985a; Chen et al., 1993). Second, laser speckle. This is inevitable with displays of the kind used here. Speckle can mask detection of interference fringes in a frequency-selective manner (Williams, 1985b). It might be argued,

therefore, that speckle may have influenced our results. We consider this unlikely for two reasons: (1) we used, for the most part, unity contrast adapting and test stimuli, and the effective contrasts of laser speckle would be insignificant in comparison; and (2) if one closely analyzes the masking effect of speckle in Williams's (1985b) data, one can see from his Figure 2 that for one observer (D.W.) speckle consistently caused twice the threshold elevation for tests below 40 c/deg as it did for tests above 40 c/deg. This could only occur if there were channels that could be differentially adapted centered at these very high frequencies—which is precisely our conclusion here. Third, intensity cues. Henning (1966) showed that observers can use the intensity of tones as cues to their pitch when discriminating between them. It is conceivable that observers could use the contrast of a fringe as a cue to its spatial frequency, and this might have influenced the results. The visual analog of Henning's forced-choice auditory experiment has not yet been performed at high spatial frequencies. However, our observers had to make matches to both the contrast *and* the spatial frequency when making matches with the method of adjustment and, thus, they could not simply make matches based on perceived contrast.

The existence of such a fine grain in the neural representation of spatial vision is even more surprising when one considers that optical losses under the best viewing conditions (2.0 mm pupil) still attenuate high-frequency components in the retinal image (>35 c/deg) by at least 70% (Campbell and Green, 1965). The contrast of high frequencies in natural images will not always make the finest channel exceed its own contrast threshold. This point should make it clear that this channel is not related to the single cone-fed receptive fields postulated by Lennie to establish chromatic opponency (Lennie, 1980; Lennie et al., 1991). Our fine channel cannot form the basis of color vision because its signal would be silenced by image blur and because color vision is patently not abolished under these conditions. The visual system did not evolve fine channels in anticipation of the development of interferometry. It will be of great interest to see, therefore, what developmental or computational constraint will emerge to explain the existence of these largely insouciant cells.

REFERENCES

- Albrecht DG, Farrar SB, Hamilton DB (1984) Spatial contrast adaptation characteristics of neurones recorded in the cat's visual cortex. *J Physiol (Lond)* 347:713–739.
- Anstis SM (1975) What does visual perception tell us about visual coding? In: *Handbook of psychobiology* (Gazzaniga MS, Blakemore C, eds), pp 267–324. New York: Academic.
- Azzopardi P, Cowey A (1993) Preferential representation of the fovea in the primary visual cortex. *Nature* 361:719–721.
- Blakemore C, Campbell FW (1969) On the existence of neurones in the human visual system selectively sensitive to the orientation and size of retinal images. *J Physiol (Lond)* 203:237–260.
- Blakemore C, Nachmias J (1971) The orientation specificity of two visual aftereffects. *J Physiol (Lond)* 213:157–174.
- Blakemore C, Sutton P (1969) Size adaptation: a new after-effect. *Science* 166:245–247.
- Blakemore C, Muncey JPI, Ridley RM (1971) Perceptual fading of a stabilized cortical image. *Nature* 233:204–205.
- Blakemore C, Muncey JPI, Ridley RM (1973) Stimulus specificity in the human visual system. *Vision Res* 13:1915–1933.
- Boycott BB, Dowling JE (1969) Organization of the primate retina: light microscopy. *Phil Trans R Soc [Biol]* 255:109–194.
- Braddick OJ, Campbell FW, Atkinson J (1978) Channels in vision: basic aspects. In: *Handbook of sensory physiology* (Held R, Leibowitz HW, Teuber HL, eds), pp 1–38. New York: Springer.
- Campbell FW, Green DG (1965) Optical and retinal factors affecting visual resolution. *J Physiol (Lond)* 181:576–593.
- Campbell FW, Robson JG (1968) Application of Fourier analysis to the visibility of gratings. *J Physiol (Lond)* 197:551–566.
- Campbell FW, Nachmias J, Jukes J (1970) Spatial-frequency discrimination in human vision. *J Opt Soc Am* 60:555–559.
- Chen B, Makous W, Williams DR (1993) Serial spatial filters in vision. *Vision Res* 33:413–427.
- Dacey DM (1993) The mosaic of midget ganglion cells in the human retina. *J Neurosci* 13:5334–5355.
- DeMonasterio FM, Gouras P (1975) Functional properties of ganglion cells of the rhesus monkey retina. *J Physiol (Lond)* 251:167–195.
- Derrington AM, Lennie P (1984) Spatial and temporal contrast sensitivities of neurones in lateral geniculate nucleus of macaque. *J Physiol (Lond)* 357:219–240.
- DeValois RL, DeValois KK (1988) *Spatial vision*. New York: Oxford UP.
- DeValois RL, Albrecht DG, Thorell LG (1977) Spatial tuning of LGN and cortical cells in monkey visual system. In: *Spatial contrast* (Sprekneise H, van der Tweel H, eds). Amsterdam: Elsevier.
- DeValois RL, Albrecht DG, Thorell LG (1982) Spatial frequency selectivity of cells in macaque visual cortex. *Vision Res* 22:545–560.
- DeValois RL, Thorell LG, Albrecht DG (1985) Periodicity of striate-cortex-cell receptive fields. *J Opt Soc Am* 2:1115–1123.
- Georgeson MA (1980) Spatial frequency analysis in early visual processing. *Phil Trans R Soc Lond [Biol]* 290:11–22.
- Georgeson MA (1985) The effect of spatial adaptation on perceived contrast. *Spatial Vis* 1:103–112.
- Graham N (1989) *Visual pattern analyzers*. New York: Oxford UP.
- Green DM, Swets JA (1966) *Signal detection theory and psychophysics*. New York: Wiley.
- Hawken MJ, Parker AJ (1991) Spatial receptive field organization in monkey V1 and its relationship to the cone mosaic. In: *Computational models of visual processing* (Landy MS, Movshon JA, eds), pp 83–93. Cambridge: MIT.
- He S, MacLeod DIA (1995) Local luminance nonlinearity and receptor aliasing in the detection of high frequency gratings. *J Opt Soc Am*, in press.
- He S, Smallman HS, MacLeod DIA (1995) Neural and cortical limits on visual resolution. *Invest Ophthalmol Vis Sci [Suppl]* 36:438.
- Henning GB (1966) Frequency discrimination of random-amplitude tones. *J Acoust Soc Am* 39:336–339.
- Hirsch J, Hylton R (1982) Limits of spatial-frequency discrimination as evidence of neural interpolation. *J Opt Soc Am* 72:1367–1374.
- Klein SA, Levi DM (1985) Hyperacuity thresholds of 1 sec: theoretical predictions and empirical validation. *J Opt Soc Am* 2:1170–1190.
- LeGrand Y (1935) Sur la mesure de l'acuité visuelle au moyen de franges d'interférence. *C R Acad Sci (Paris)* 200:490–491.
- Lennie P (1980) Parallel visual pathways: a review. *Vision Res* 20:561–594.
- Lennie P, Haake PW, Williams DR (1991) The design of chromatically opponent receptive fields. In: *Computational models of visual processing* (Landy MS, Movshon JA, eds), pp 71–82. Cambridge: MIT.
- Määttänen LM, Koenderink JJ (1991) Contrast adaptation and contrast gain control. *Exp Brain Res* 87:205–212.
- MacLeod DIA, He S (1993) Visible flicker from invisible flickering lights. *Nature* 361:256–258.
- MacLeod DIA, Williams DR, Makous W (1992) A visual nonlinearity fed by single cones. *Vision Res* 32:347–363.
- Maffei L, Fiorentini A, Bisti S (1973) Neural correlate of perceptual adaptation to gratings. *Science* 182:1036–1038.
- Marr D, Poggio T, Hildreth E (1980) Smallest channel in early human vision. *J Opt Soc Am* 70:868–870.
- McMahon MJ, Lankheet MJM, Lennie P, Williams DR (1995) Fine structure of P-cell receptive fields in the fovea revealed by laser interferometry. *Invest Ophthalmol Vis Sci [Suppl]* 36:4.
- Miller WH, Bernard GD (1983) Averaging over the foveal receptor aperture curtains aliasing. *Vision Res* 23:1365–1369.
- Morgan MJ, Ward RM (1985) Spatial and spatial-frequency primitives in spatial-interval discrimination. *J Opt Soc Am* 2:1205–1210.
- Movshon JA, Lennie P (1979) Pattern-selective adaptation in visual cortical neurones. *Nature* 278:850–852.
- Ohzawa I, Sclar G, Freeman RD (1985) Contrast gain control in the cat's visual system. *J Neurophysiol* 54:651–667.
- Parker AJ, Hawken MJ (1985) Capabilities of monkey cortical cells in spatial-resolution tasks. *J Opt Soc Am* 2:1101–1114.

- Perry VH, Cowey A (1985) The ganglion cell and cone distributions in the monkey's retina: implications for central magnification factors. *Vision Res* 25:1795–1810.
- Polyak SL (1941) *The retina*. Chicago: University of Chicago.
- Raviola E, Gilula NB (1973) Gap junctions between photoreceptor cells in the vertebrate retina. *Proc Natl Acad Sci USA* 70:1677–1681.
- Regan D, Beverley KI (1983) Spatial-frequency discrimination and detection: comparison of postadaptation thresholds. *J Opt Soc Am* 73:1684–1690.
- Regan D, Bartol S, Murray TJ, Beverley KI (1982) Spatial frequency discrimination in normal vision and in patients with multiple sclerosis. *Brain* 105:735–754.
- Schein SJ (1988) Anatomy of macaque fovea and spatial densities of neurons in foveal representation. *J Comp Neurol* 269:479–505.
- Smallman HS, MacLeod DIA (1994) Paradoxical effects of adapting to large disparities: constraining population code models of disparity. *Invest Ophthalmol Vis Sci [Suppl]* 35:1917.
- Tsukamoto Y, Masarachia P, Schein SJ, Sterling P (1992) Gap junctions between the pedicles of macaque foveal cones. *Vision Res* 32:1809–1815.
- Watson AB (1982) Summation of grating patches indicates many types of detector at one retinal location. *Vision Res* 22:17–26.
- Watson AB (1983) Detection and recognition of simple spatial forms. In: *Physical and biological processing of images* (Braddick OJ, Sleigh AC, eds), pp 100–114. Berlin: Springer.
- Watt RJ, Morgan MJ (1985) A theory of the primitive spatial code in human vision. *Vision Res* 25:1661–1674.
- Westheimer G (1981) Visual hyperacuity. *Prog Sens Physiol* 1:1–30.
- Williams DR (1985a) Aliasing in human foveal vision. *Vision Res* 25:195–205.
- Williams DR (1985b) Visibility of interference fringes near the resolution limit. *J Opt Soc Am* 2:1087–1093.
- Williams DR (1988) Topography of the foveal cone mosaic in the living human eye. *Vision Res* 28:433–454.
- Williams DR, Brainard DH, McMahon MJ, Navarro R (1994) Double-pass and interferometric measures of the optical quality of the eye. *J Opt Soc Am* 11:3123–3135.
- Wilson HR (1986) Response of spatial mechanisms can explain hyperacuity. *Vision Res* 26:453–469.
- Wilson HR (1991) Psychophysical models of spatial vision and hyperacuity. In: *Spatial vision* (Regan D, ed), pp 64–86. Boca Raton, FL: CRC.
- Wilson HR, Gelb DJ (1984) Modified line element theory for spatial frequency and width discrimination. *J Opt Soc Am* 1:124–131.
- Wilson HR, Humanski R (1993) Spatial frequency adaptation and contrast gain control. *Vision Res* 33:1133–1149.
- Wilson HR, McFarlane DK, Phillips GC (1983) Spatial frequency tuning of orientation selective units estimated by oblique masking. *Vision Res* 23:873–882.
- Wilson HR, Levi D, Maffei L, Rovamo J, DeValois RL (1990) The perception of form: retina to striate cortex. In: *Visual perception: the neurophysiological foundations* (Spillman L, Werner JS, eds), pp 317–347. San Diego: Academic.
- Yager D, Kramer P (1991) A model for perceived spatial frequency and spatial frequency discrimination. *Vision Res* 31:1067–1072.